Available online at www.sciencedirect.com
ScienceDirect
Journal of Sound and Vibration 306 (2007) 657–674
JOURNAL OF SOUND AND VIBRATION
www.elsevier.com/locate/jsvi

An asymptotic analysis for the coupled dispersion characteristics of a structural acoustic waveguide

Abhijit Sarkar, Venkata R. Sonti*

Facility for Research in Technical Acoustics, Department of Mechanical Engineering, Indian Institute of Science, Bangalore 560 012, India

Received 15 December 2006; received in revised form 7 May 2007; accepted 2 June 2007

Abstract

Analytical expressions are derived, using asymptotics, for the fluid–structure coupled wavenumbers in a one-dimensional (1-D) structural acoustic waveguide. The coupled dispersion equation of the system is rewritten in the form of the uncoupled dispersion equation with an added term due to the fluid–structure coupling. As a result of this coupling, the prior uncoupled structural and acoustic wavenumbers, now become coupled structural and acoustic wavenumbers. A fluid-loading parameter ε, defined as the ratio of mass of fluid to mass of the structure per unit area, is introduced which when set to zero yields the uncoupled dispersion equation. The coupled wavenumber is then expressed in terms of an asymptotic series in ε. Analytical expressions are found as ε is varied from small to large values. Different asymptotic expansions are used for different frequency ranges with continuous transitions occurring between them. This systematic derivation helps to continuously track the wavenumber solutions as the fluid-loading parameter is varied from small to large values. Though the asymptotic expansion used is limited to the first-order correction factor, the results are close to the numerical results. A general trend is that a given wavenumber branch transits from a rigid-walled solution to a pressure-release solution with increasing ε. Also, it is found that at any frequency where two wavenumbers intersect in the uncoupled analysis, there is no more an intersection in the coupled case, but a gap is created at that frequency.

1. Introduction

In structural acoustics, one of the many relevant questions is how a wavenumber of a structure vibrating in vacuum changes when placed in contact with (or immersed in) a fluid and also how the acoustical wavenumber in an infinite domain (or inside a rigid-walled waveguide) modifies when in contact with (or enclosed by) a flexible structure. The common way of investigating these two questions is to derive a fluid–structure coupled dispersion relation and find the modified wavenumbers (numerically or analytically).

Fluid–structure interaction where the fluid domain is infinite is quite different in its characteristics from that where the fluid is enclosed by a flexible structure. Our focus in this study shall be a system where the fluid is enclosed in a 1-D flexible-walled waveguide. As the literature survey section will show, several relevant studies exist where coupled wavenumber results have been presented for systems such as fluid-filled rectangular ducts and cylindrical shells. These studies have used numerical methods in obtaining the solution.

*Corresponding author. Tel.: +91 080 2293 3227.
E-mail address: sonti@mecheng.iisc.ernet.in (V.R. Sonti).

0022-460X/$ - see front matter © 2007 Elsevier Ltd. All rights reserved.
doi:10.1016/j.jsv.2007.06.005

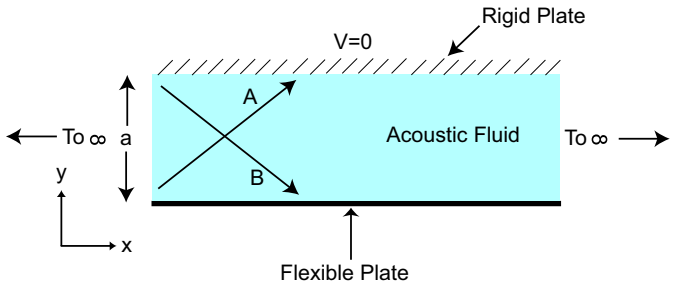

Fig. 1. Schematic showing the flexible plate with the column of acoustic fluid having a rigid cover plate at the top.

It would, however, be useful if one could derive analytical expressions for the coupled wavenumbers (as opposed to numerical solutions) so that the physics can be brought out readily and the expressions themselves could be of use in design. Asymptotic methods offer such means of arriving at the analytical expressions. For example, the coupled dispersion equation can be expressed as the *in vacuo* structural dispersion equation with a correction term due to the fluid. One could then find a perturbed solution to the structural wavenumber around the *in vacuo* solution. A similar approach can be used for the acoustical wavenumber also with a correction term due to the flexible structure. The analytical expression directly gives the shift in the uncoupled wavenumber due to the coupling. Thus, one can understand the wavenumber shift as being due to a stiffness-like or an inertia-like effect of the structure/fluid on the fluid/structure, respectively. Such information can be useful for a practicing engineer in understanding shifts of resonances in finite structural acoustic systems due to fluid–structure coupling.

In this article, the system considered is a flexible infinite plate (in the xz plane) in contact with a fluid column of height a (in the y-direction). The top of the fluid column is covered with a rigid plate (at $y = a$) (see Fig. 1). We assume that all physical quantities are independent of z. The x-direction flexural plate wavenumber gets influenced by the presence of the fluid column and so also the acoustical wavenumber in the fluid modifies due to the flexible plate. This coupling effect is represented by a fluid-loading parameter ε (to be defined later). Asymptotic expressions for the coupled wavenumbers of the system described above are derived, first for small and then for large ε values.

2. Literature survey

In the present section we briefly review earlier works of similar nature. In the later part of the article we shall compare our results with some of the results reported in these references.

This problem is identical to that analysed by Fahy [1]. Instead of the rigid cover plate at $y = a$, he considered another identical flexible plate at $y = 2a$ and analysed symmetric modes only. Under the symmetry assumption, this implies that the y-direction velocity is zero at the centerline $y = a$, which is exactly our model. We shall analyse the problem in a greater detail. While Fahy has presented numerical solutions, these solutions cannot be traced from their uncoupled counterparts. Our approach being based on analytical expressions such tracing is possible, bringing useful insights to the solutions.

An early experimental investigation of sound propagation through flexible cylindrical pipes was carried on by Kerschen and Johnston [2]. It was observed that the modal contribution of each cut-on mode encounters a dip at the frequency where the axial phase speed of the cut-on mode coincides with the flexural wave speed of the structural material. They concluded that at these frequencies, the dip in the modal contribution was due to the energy being carried by the structural vibrations. Cabelli [3] studied the dispersion characteristics of an infinite duct with a square cross-section with one flexible wall clamped at the edges. A mode summation procedure was adopted for this purpose. A numerical solution was presented for the coupled dispersion characteristics by truncating the summation to a finite number of terms. Experimental study on sound propagation in a flexible membrane duct was carried by Huang et al. [4]. A theoretical model in support of their experimental result was also presented. A further generalised study by Ko [5] included mean flow effects

in a 2-D acoustic duct bounded by a flexural beam on one side. He theoretically found the axial phase velocities for various acoustic modes. He concluded that the phase velocities are not greatly affected if the acoustic wave propagation is in the direction of bulk flow. However, large changes were observable in case the acoustic wave propagation is in the direction opposite to that of the bulk flow. Experimental studies on flexible membrane ducts including fluid flow effects were presented by Choi and Kim [6]. Coupled dispersion characteristics for fluid-filled cylindrical pipes was presented by Fuller and Fahy [7]. They used a numerical solution methodology in solving the coupled dispersion equation. They performed studies for different values of shell thickness to radius ratio and also used different material combinations. The behaviour of various branches of the dispersion curve under the influence of these parameters was discussed in their article. Pavic [8] in his study of vibrational energy flow in a cylindrical shell also obtained the dispersion curves of a fluid-filled cylindrical shell. Au-Yang [9] studied a model of coaxial cylinders with fluid filled in the annular region and the outer cylinder being rigid. He presented the hydrodynamic mass perceived by the structure due to the presence of the fluid.

Asymptotic analysis has been widely prevalent in solving a wide realm of problems. Excellent treatises are available which introduce the subject [10,11]. The use of asymptotic analysis methodology in analysing the coupled structural-acoustic problem as a perturbation over the *in vacuo* structural dynamics and the uncoupled acoustic problem was elaborated in the classic text by Morse and Ingard [12]. Later, Crighton [13,14] developed this methodology further. Morse and Ingard as also Crighton used asymptotic analysis in the context of external fluid of infinite extent. Further work in this direction is being carried by Peake and Sorokin [15] and Chapman and Sorokin [16]. In the present article, we use the asymptotic method similar to Crighton [13] in studying the coupled structural acoustics problem when the fluid in contact with the structure is of finite extent. In contrast to the external unbounded fluid domain, the complication of branch-cuts does not arise for the case of bounded fluid domains. However, in the latter case the cut-on effects arise.

In the following sections, a detailed derivation of the dispersion relation for the system shown in Fig. 1 is presented.

3. The dispersion relation

We begin with the derivation of the dispersion equation for our model. In our approach, frequency is kept as an independent variable and the coupled wavenumber will be found as a function of frequency. At a circular frequency ω, the acoustic pressure in the fluid is described by the acoustic wave equation in 2-D Cartesian coordinates given by

$$\frac{\partial^2 p(x,y,t)}{\partial x^2}+\frac{\partial^2 p(x,y,t)}{\partial y^2}=\frac{1}{c^2}\frac{\partial^2 p(x,y,t)}{\partial t^2}, \tag{1}$$

which has the solution of the form (see Ref. [1] for detailed derivation):

$$p(x,y,t)=A\mathrm{e}^{\mathrm{i}(\omega t-k_x x-k_y y)}+B\mathrm{e}^{\mathrm{i}(\omega t-k_x x+k_y y)}, \tag{2}$$

where k_x is the wavenumber in the x-direction, k_y is the wavenumber in the y-direction. Also, we have the relation $k_x^2+k_y^2=k^2=\omega^2/c^2$, where k is the acoustic wavenumber and c the sonic velocity of the acoustic medium.

The governing differential equation for the transverse displacement (in the y-direction) $w(x)$ of the plate at a frequency ω is (due to independence of all quantities in the z-direction, all partial derivatives with respect to z vanish)

$$\frac{Eh^3}{12(1-\nu^2)}\frac{\mathrm{d}^4 w(x)}{\mathrm{d}x^4}-\rho_p h\omega^2 w(x)=-p(x,0), \tag{3}$$

where E is the modulus of elasticity, ρ_p the beam density, h the thickness of the beam, ν the Poisson's ratio of the plate material and $m=\rho_p h$ is the mass per unit length of the beam of unit width (see Ref. [1] for details). We shall use I to denote the quantity $h^3/(12(1-\nu^2))$.

The acoustic pressure and velocity in the y-direction are related by

$$-\mathrm{i}\omega\rho v(x,y)=\frac{\partial p(x,y)}{\partial y}, \tag{4}$$

where ρ is the fluid density and v the acoustic velocity in the y-direction.

At the structure–fluid interface ($y=0$), the condition of velocity continuity results in $v(x,0)=\mathrm{i}\omega w(x)$. Applying Eq. (4) at $y=0$ and using the above velocity continuity condition we have

$$\omega^2\rho w(x)=\left[\frac{\partial p(x,y)}{\partial y}\right]_{y=0}=(-\mathrm{i}k_yA+\mathrm{i}k_yB)\mathrm{e}^{-\mathrm{i}k_xx}. \tag{5}$$

At $y=a$, the zero velocity due to the rigid cover plate and Eq. (4) give

$$(-\mathrm{i}k_yA\mathrm{e}^{-\mathrm{i}k_ya}+\mathrm{i}k_yB\mathrm{e}^{\mathrm{i}k_ya})\mathrm{e}^{-\mathrm{i}k_xx}=0\Rightarrow A=B\mathrm{e}^{\mathrm{i}2k_ya}. \tag{6}$$

From Eqs. (5) and (6), we thus have

$$w(x)=\frac{B\mathrm{i}k_y\mathrm{e}^{-\mathrm{i}k_xx}(1-\mathrm{e}^{\mathrm{i}2k_ya})}{\omega^2\rho}. \tag{7}$$

Eq. (3) now becomes

$$(EIk_x^4-\omega^2m)w(x)=-B\mathrm{e}^{-\mathrm{i}k_xx}(1+\mathrm{e}^{\mathrm{i}2k_ya}). \tag{8}$$

Let the *in vacuo* bending wavenumber be denoted by $k_b=\left(m\omega^2/EI\right)^{1/4}$. Using Eq. (7), Eq. (8) becomes

$$(EIk_x^4-\omega^2m)\frac{\mathrm{i}k_y(1-\mathrm{e}^{\mathrm{i}2k_ya})}{\omega^2\rho}=-(1+\mathrm{e}^{\mathrm{i}2k_ya})\Rightarrow(EIk_x^4-\omega^2m)=-\frac{\omega^2\rho}{k_y}\cot(k_ya). \tag{9}$$

Further rearrangement leads to

$$k_x^4-k_b^4=-\frac{k_b^4\rho a}{m}\frac{\cot(k_ya)}{k_ya}\Rightarrow\frac{k_x^4}{k_b^4}=\left[1-\left(\frac{\rho a}{m}\right)\frac{\cot(k_ya)}{k_ya}\right]. \tag{10}$$

Eq. (10) is non-dimensionalized with respect to the coincidence frequency (ω_c) and the wavenumber at coincidence (k_c) to give the following non-dimensional coupled dispersion relation for the structural-acoustic system:

$$\left[\frac{\xi^4}{\Omega^2}-1\right]\left[\lambda\sqrt{\Omega^2-\xi^2}\,\tan\left(\lambda\sqrt{\Omega^2-\xi^2}\right)\right]+\varepsilon=0. \tag{11}$$

The non-dimensional parameters are explained in Table 1.

The coincidence frequency (ω_c) appearing in the non-dimensionalization process is defined (as in Fahy [1]) as the frequency at which the wavenumber of the *in vacuo* plate equals the wavenumber of the uncoupled plane

Table 1
Non-dimensional parameters used in Eq. (10) to arrive at Eq. (11)

Non-dimensional parameters	Physical description
$\Omega=\dfrac{\omega}{\omega_c}=\dfrac{k}{k_c}$	Non-dimensional frequency
$\lambda=k_ca$	Non-dimensional fluid column height
$\varepsilon=\dfrac{\rho a}{m}$	Fluid loading parameter
$\xi=\dfrac{k_x}{k_c}$	Coupled wavenumber non-dimensionalized with respect to the coincidence wavenumber
$\chi=\dfrac{k_x}{k}=\dfrac{\xi}{\Omega}$	Coupled wavenumber non-dimensionalized with respect to the acoustic wavenumber

acoustic wave. Thus, we have the following relation:

$$\sqrt[4]{\frac{m\omega_c^2}{EI}} = \frac{\omega_c}{c} \Rightarrow \omega_c = c^2\sqrt{\frac{m}{EI}} \quad \text{and} \quad k_c = \frac{\omega_c}{c} = c\sqrt{\frac{m}{EI}}. \tag{12}$$

Eq. (9) is the *in vacuo* beam equation with an added term on the right side due to fluid loading. For the coupled structural wavenumber (k_x), we look for perturbations to the *in vacuo* wavenumber k_b. Similar to the *in vacuo* structural wavenumber which modifies due to the presence of the acoustic medium, the plane wave and cut-on acoustic wavenumbers modify due to the fluid–structure coupling. This modification of the acoustic wavenumber can be looked upon as due to a change from a zero velocity boundary condition (very hard structure) or a zero pressure-boundary condition (very soft structure) to a boundary condition caused by a structure with finite flexibility. From the next section, we begin deriving the asymptotic expressions for these coupled wavenumbers (structural and acoustic). Coupled wavenumbers for small values of the fluid-loading parameter ε will be presented first in Section 4 followed by Section 5 for large values of ε.

4. Small fluid-loading parameter

Eq. (11) is rewritten below, where the first square bracketed term is identified as the structural dispersion relation and the second bracketed term corresponds to the acoustic dispersion relation:

$$\overbrace{\left[\frac{\xi^4}{\Omega^2} - 1\right]}^{\text{Structure}} \left[\underbrace{\lambda\sqrt{\Omega^2 - \xi^2}}_{\text{Acoustic plane wave}} \quad \overbrace{\tan\left(\lambda\sqrt{\Omega^2 - \xi^2}\right)}^{\text{Rigid duct cut-on}}\right] + \varepsilon = 0.$$

In the equation above, the condition $\varepsilon = \rho a/m = 0$ corresponds to a zero-density ambient fluid for the structure and also to an infinitely dense structure as seen by the fluid. The solutions in that case, correspond to the *in vacuo* structural wavenumber, the wavenumber of the plane acoustic wave and the wavenumber of the rigid-duct acoustic cut-on (with velocity zero on the edges $y = 0$ and $y = a$), respectively. These wavenumbers can be obtained by equating each of the bracketed expressions in the above equation to zero, resulting in

$$\xi = \Omega^{1/2}, \tag{13a}$$

$$\xi = \Omega, \tag{13b}$$

$$\lambda^2(\Omega^2 - \xi^2) = n^2\pi^2 \Rightarrow \xi = \sqrt{\Omega^2 - \frac{n^2\pi^2}{\lambda^2}} \text{ where } n = 1, 2, 3, \ldots \tag{13c}$$

Eqs. (13a), (13b) and (13c) in the dimensional form are $k_x = \sqrt{kk_c}$, $k_x = k$ and $k_x = \sqrt{k^2 - (n^2\pi^2)/\lambda^2}$, respectively. These solutions are presented in Fig. 2 for $\lambda = 3$.

Instead of $\varepsilon = 0$, when $0 < \varepsilon \ll 1$, the solutions of ξ are expected to be perturbations to Eqs. (13a), (13b) and (13c). These perturbed solutions will be denoted by $\xi_s(\varepsilon)$, $\xi_a(\varepsilon)$ and $\xi_a^n(\varepsilon)$, respectively. The functions $\xi_s(\varepsilon)$, $\xi_a(\varepsilon)$, $\xi_a^n(\varepsilon)$ will be such that with $\varepsilon = 0$ these reduce to the expressions in Eqs. (13a), (13b) and (13c). Thus, $\xi_s(\varepsilon)$ is a perturbation to the *in vacuo* structural wavenumber, while $\xi_a(\varepsilon)$ is a perturbation to the wavenumber of the acoustic plane wave. In this article we shall use the phrases, ''coupled structural wavenumber'', and ''coupled acoustic wavenumber'', respectively, while referring to them. Similarly, $\xi_a^n(\varepsilon)$ shall refer to the perturbed wavenumber of the nth cut-on mode of the rigid-walled acoustic duct (zero velocities at both edges).

For the sake of clarity, a schematic of the results to be found later is presented here in Fig. 3. The schematic shows all the wavenumber branches for which asymptotic expressions will be derived in the following subsections. The asymptotic expressions derived in each subsection shall be valid only for particular frequency ranges. Each derivation shall be accompanied by an inset picture identical to that of Fig. 3, where the applicable portion of the branch shall be marked in bold.

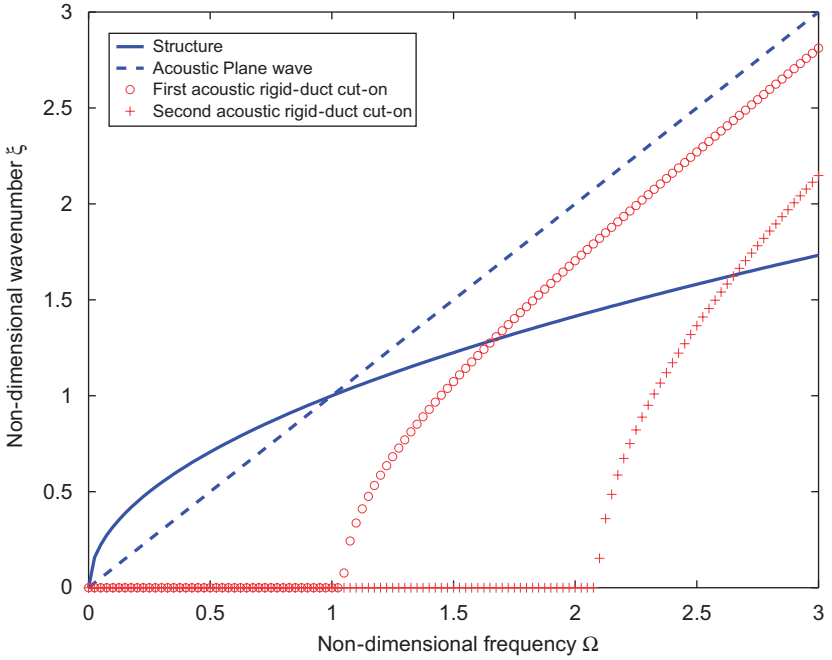

Fig. 2. The uncoupled solutions of Eq. (11) with $\varepsilon = 0$.

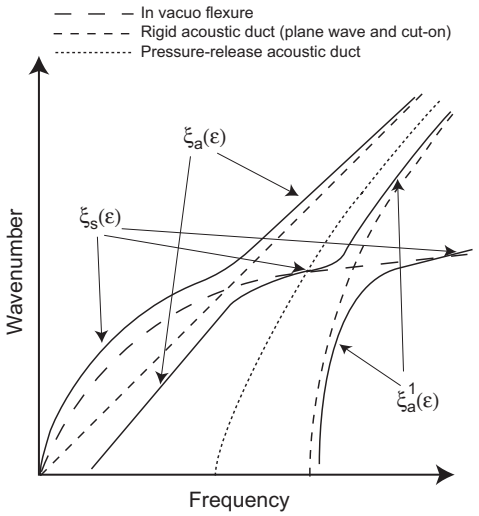

Fig. 3. Schematic of the coupled wavenumber solutions for small values of the fluid-loading parameter.

4.1. $\xi_s(\varepsilon)$

In order to find $\xi_s(\varepsilon)$, we assume $\xi = \Omega^{1/2} + a_1\varepsilon + a_1\varepsilon^2$. Substituting this expression for ξ in Eq. (11) and performing a series expansion about $\varepsilon = 0$ we get $\xi_s(\varepsilon)$ (see Table 2).

From Table 2 the following inferences may be drawn:

- For $\Omega < 1$, since the correction term always remains positive, $\xi_s(\varepsilon) > \xi_s(0) = \sqrt{\Omega}$. Thus, at frequencies below coincidence, due to the presence of the fluid, the structural wavenumber increases over its *in vacuo* value. As the structural wavenumber is proportional to $\sqrt{m}$, this denotes mass loading on the structure due to the presence of the fluid. Also, due to the coth term, the correction becomes large at $\Omega \approx 1$ or 0, making the

Table 2
Derivation of the asymptotic expression for $\xi_s(\varepsilon)$

Substituting $\xi = \Omega^{1/2} + a_1\varepsilon + a_2\varepsilon^2$ in Eq. (11) and performing a series expansion about ε we get

$$\left(4\frac{a_1\lambda\sqrt{\Omega^2-\Omega}\tan\left(\lambda\sqrt{\Omega^2-\Omega}\right)}{\sqrt{\Omega}}+1\right)\varepsilon+\mathcal{O}(\varepsilon^2)=0.$$

Equating terms at $\mathcal{O}(\varepsilon)$ we get $a_1 = -\frac{1}{4}\frac{\sqrt{\Omega}}{\lambda\sqrt{\Omega^2-\Omega}\tan\left(\lambda\sqrt{\Omega^2-\Omega}\right)}$. Hence,

$$\text{If } \Omega>1, \quad \xi_s(\varepsilon)=\sqrt{\Omega}\left[1-\underbrace{\frac{\varepsilon}{4}\frac{\cot\left(\lambda\sqrt{\Omega^2-\Omega}\right)}{\lambda\sqrt{\Omega^2-\Omega}}}_{\text{correction}}\right]. \tag{14}$$

$$\text{If } \Omega<1, \quad \xi_s(\varepsilon)=\sqrt{\Omega}\left[1+\underbrace{\frac{\varepsilon}{4}\frac{\coth\left(\lambda\sqrt{\Omega-\Omega^2}\right)}{\lambda\sqrt{\Omega-\Omega^2}}}_{\text{correction}}\right]. \tag{15}$$

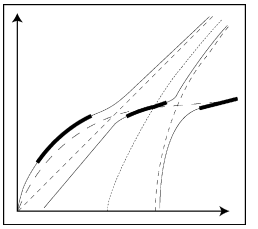

asymptotic expression invalid at these frequencies. A different form of expansion needs to be used to find a valid expression at these frequencies. This will be presented later in this article.

- For $\Omega>1$, due to the presence of the cot term, the correction term alternates from positive to negative values about frequencies Ω where $\lambda\sqrt{\Omega^2-\Omega} = ((2n+1)\pi)/2$, $(n=0,1,2,\ldots)$. Immediately beyond coincidence, the correction term is positive. A positive correction indicates that $\xi_s(\varepsilon)$ is less than the *in vacuo* value $\xi_s(0)$ and hence the fluid loading is in the form of stiffness. A negative correction indicates that $\xi_s(\varepsilon)$ is more than the *in vacuo* value $\xi_s(0)$ and hence the fluid loading is in the form of mass. Thus, the fluid loading alternates between stiffness and inertia in alternate frequency bands. A spring-mass system backed by an acoustic cavity has a similar nature of fluid loading [1].

The derived expression in Eq. (14) is invalid for frequencies Ω such that $\lambda\sqrt{\Omega^2-\Omega}\approx n\pi$. These frequencies occur for $\Omega\approx 0$, $\Omega\approx 1$ and $\Omega_c^n = \left(1/2\lambda + 1/2\sqrt{\lambda^2+4n^2\pi^2}\right)/\lambda$, $(n=1,2,3,\ldots)$. For these frequencies, a different set of expansions will be derived later. Note, that Ω_c^n is the frequency at which the *in vacuo* structural dispersion curve intersects the dispersion curve of the nth cut-on mode of the rigid acoustic duct.

4.2. $\xi_a(\varepsilon)$

The detailed derivation for $\xi_a(\varepsilon)$ is presented in Table 3.
From Eq. (16) the following inferences may be drawn:

- For $\Omega<1$, the correction term indicated by the underbraces is negative and thus, $\xi_a(\varepsilon)$ is lesser than $\xi_a(0)$. The asymptotic solution turns invalid for $\Omega\approx 1$ and $\Omega\approx 0$.
- For $\Omega>1$, the correction term indicated by the underbraces is positive and thus, $\xi_a(\varepsilon)$ is greater than $\xi_a(0)$. The asymptotic solution turns invalid for $\Omega\approx 1$.
- For large Ω the correction term decreases. Thus, as the frequency increases, the solution approaches (but remains greater than) the wavenumber of the acoustic plane wave.

In Fig. 4, are plotted $\xi_s(\varepsilon)$ and $\xi_a(\varepsilon)$ using the derived relations in Tables 2 and 3 with $\lambda = 3$ and $\varepsilon = 0.25$. Overlaid on the plot are the *in vacuo* structural dispersion curve (in dashed line) and the plane wave acoustic dispersion curve (in dash–dot line). The asymptotic solutions can be seen to be perturbations of the uncoupled

Table 3
Derivation of the asymptotic expression for $\xi_a(\varepsilon)$

Substituting $\xi = \Omega + a_1\varepsilon + a_2\varepsilon^2$ in Eq. (11) and performing a series expansion about ε we get

$$\left(-2(\Omega^2-1)\lambda^2\Omega a_1 + 1\right)\varepsilon + \mathcal{O}(\varepsilon^2) = 0.$$

Equating terms at $\mathcal{O}(\varepsilon)$ we get $a_1 = \frac{1}{2}\frac{1}{(\Omega^2-1)\lambda^2\Omega}$. Hence,

$$\xi_a(\varepsilon) = \Omega\left[1 + \underbrace{\frac{1}{2}\frac{\varepsilon}{(\Omega^2-1)\lambda^2\Omega^2}}_{\text{correction}}\right]. \tag{16}$$

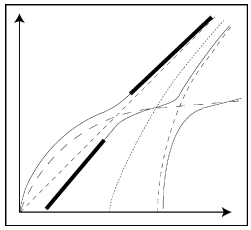

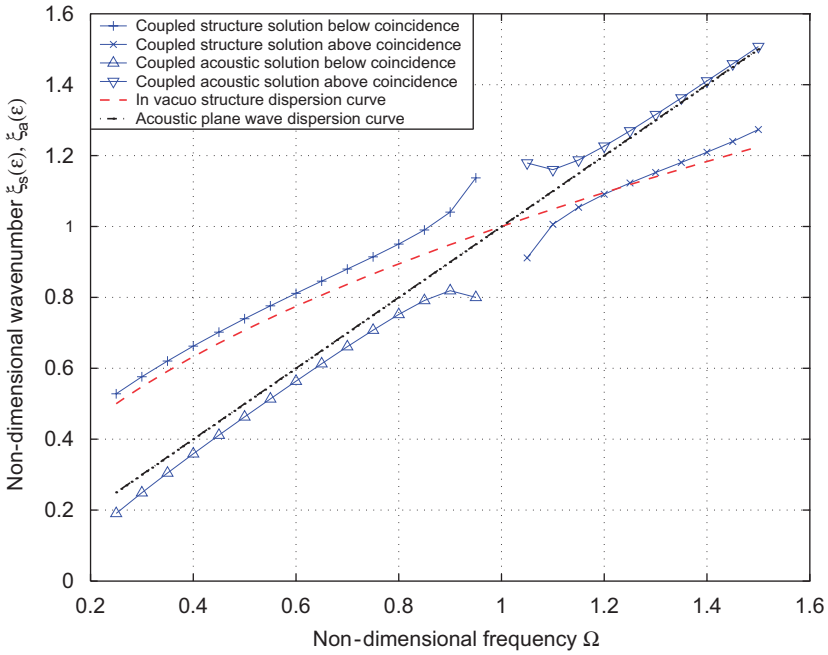

Fig. 4. Coupled structural and acoustic plane wave solutions of Eq. (11) with $\lambda = 3$, $\varepsilon = 0.25$.

solutions. The coupled acoustic plane wave solution beyond coincidence is seen to approach the linear acoustic plane wave dispersion curve as the frequency increases. Also, the figure shows that these solutions blow up near the coincidence region. An alternative solution around $\Omega \approx 1$ is found in the next subsection for both $\xi_s(\varepsilon)$ and $\xi_a(\varepsilon)$.

4.3. $\xi_s(\varepsilon)$ and $\xi_a(\varepsilon)$ (near $\Omega = 1$)

For solutions near $\Omega = 1$, we substitute $\Omega = 1 + \varepsilon\Psi$ in Eq. (11), where Ψ is an $\mathcal{O}(1)$ quantity positive or negative. To find $\xi_a(\varepsilon)$, we use a substitution $\xi = \Omega + a_1\varepsilon + a_2\varepsilon^2$ and perform a series expansion about $\varepsilon = 0$, obtaining $\varepsilon - 2(2\Psi + 4a_1)\lambda^2 a_1\varepsilon^2 + \mathcal{O}(\varepsilon^3) = 0$. It is not possible to balance this series at $\mathcal{O}(\varepsilon)$. Thus, a different

Table 4
Derivation for $\xi_s(\varepsilon)$ and $\xi_a(\varepsilon)$ near the coincidence frequency

Substituting $\xi = \Omega + a_1\varepsilon^\beta + a_2\varepsilon^{2\beta}$ in Eq. (11) and performing a series expansion about $\varepsilon = 0$ we get the following order relations for the terms in Eq. (11)

$$\frac{\xi^4}{\Omega^2} - 1 \approx \frac{\Omega^4 + 4\Omega^3\varepsilon^\beta - \Omega^2}{\Omega^2} = \mathcal{O}(\varepsilon^\beta) \quad (\text{since } \Omega = \mathcal{O}(1)),$$

$$\Omega^2 - \xi^2 = \mathcal{O}(\varepsilon^\beta) \Rightarrow \sqrt{\Omega^2 - \xi^2} = \mathcal{O}(\varepsilon^{\beta/2}) \Rightarrow \tan\left(\lambda\sqrt{\Omega^2 - \xi^2}\right) = \mathcal{O}(\varepsilon^{\beta/2}),$$

$$\left[\frac{\xi^4}{\Omega^2} - 1\right]\left[\lambda\sqrt{\Omega^2 - \xi^2}\tan\left(\lambda\sqrt{\Omega^2 - \xi^2}\right)\right] = \mathcal{O}(\varepsilon^{2\beta}).$$

Hence, for order balance it is required to have $\beta = \frac{1}{2}$. Using $\xi = \Omega + a_1\varepsilon^{1/2} + a_2\varepsilon$ in Eq. (11) and performing a series expansion about $\varepsilon = 0$, we get $(-8\lambda^2 a_1^2 + 1)\varepsilon + \mathcal{O}(\varepsilon^{3/2}) = 0$. Equating terms at $\mathcal{O}(\varepsilon)$, we get $a_1 = \pm\frac{1}{4}\frac{\sqrt{2}}{\lambda}$. Thus, we have $\xi_a(\varepsilon)$ near coincidence frequency given by

$$\xi_a(\varepsilon) = \Omega \pm \frac{\sqrt{2\varepsilon}}{4\lambda}. \tag{17}$$

Similarly, using $\xi = \sqrt{\Omega} + a_1\varepsilon^{1/2} + a_2\varepsilon$ in Eq. (11) gives $\xi_s(\varepsilon)$ near coincidence frequency as

$$\xi_s(\varepsilon) = \sqrt{\Omega} \pm \frac{\sqrt{2\varepsilon}}{4\lambda}. \tag{18}$$

The proper sign of the correction terms in Eqs. (17) and (18) will be fixed from physical arguments. From Tables 2 and 3 (as also Fig. 4) for frequencies below coincidence we have $\xi_a(\varepsilon) < \xi_a(0)$ and $\xi_s(\varepsilon) > \xi_s(0)$, while for frequencies above coincidence, we have $\xi_a(\varepsilon) > \xi_a(0)$ and $\xi_s(\varepsilon) < \xi_s(0)$. Thus, to attain a continuous transition at the coincidence region the following sign choice is necessary

$$\xi_s(\varepsilon) = \sqrt{\Omega} + \frac{\sqrt{2\varepsilon}}{4\lambda} \quad \text{when } \Omega \approx <1, \tag{19a}$$

$$\xi_s(\varepsilon) = \sqrt{\Omega} - \frac{\sqrt{2\varepsilon}}{4\lambda} \quad \text{when } \Omega \approx >1, \tag{19b}$$

$$\xi_a(\varepsilon) = \Omega - \frac{\sqrt{2\varepsilon}}{4\lambda} \quad \text{when } \Omega \approx <1, \tag{19c}$$

$$\xi_a(\varepsilon) = \Omega + \frac{\sqrt{2\varepsilon}}{4\lambda} \quad \text{when } \Omega \approx >1. \tag{19d}$$

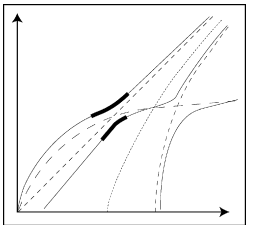

series expansion for ξ needs to be found. For this we have to resort to an order balance argument. The steps are shown in Table 4.

Note, $\xi_s(\varepsilon) \to 1 + \left(\sqrt{2\varepsilon}/4\lambda\right)$ as $\Omega \to 1^-$ and $1 - \left(\sqrt{2\varepsilon}/4\lambda\right)$ as $\Omega \to 1^+$ while $\xi_a(\varepsilon) \to 1 - \left(\sqrt{2\varepsilon}/4\lambda\right)$ as $\Omega \to 1^-$ and $1 + \left(\sqrt{2\varepsilon}/4\lambda\right)$ as $\Omega \to 1^+$. Thus, each branch encounters a *jump* of $\sqrt{2\varepsilon}/2\lambda$ at $\Omega = 1$. Alternatively, at $\Omega = 1$, the $\xi_s(\varepsilon)$ branch for $\Omega < 1$ becomes continuous with the $\xi_a(\varepsilon)$ branch for $\Omega > 1$, the common value being $1 + \left(\sqrt{2\varepsilon}/4\lambda\right)$. Similarly, the $\xi_a(\varepsilon)$ branch for $\Omega < 1$ becomes continuous with the $\xi_s(\varepsilon)$ branch for $\Omega > 1$, the common value being $1 - \left(\sqrt{2\varepsilon}/4\lambda\right)$. Thus, the coupled dispersion curves do not intersect each other at the coincidence frequency but create a gap in the region.

4.4. $\xi_s(\varepsilon)$ (near $\Omega = 0$)

It was observed that the coupled structural wavenumber given by Eq. (14) breaks down near $\Omega = 0$. An alternative solution for $\xi_s(\varepsilon)$ valid around $\Omega = 0$ will be derived in this subsection. Since the plane acoustic

wave shows a cut-on at a frequency of $\mathcal{O}(\sqrt{\varepsilon})$ (see derivation in Ref. [1]), no separate solution for $\xi_a(\varepsilon)$ near $\Omega = 0$ needs to be found.

For finding $\xi_s(\varepsilon)$, we substitute $\Omega = \varepsilon\Psi$, and $\xi = \sqrt{\varepsilon\Psi} + a_1\sqrt{\varepsilon} + a_2\varepsilon$ in Eq. (11). After performing a series expansion, the following equation is obtained at $\mathcal{O}(\varepsilon)$:

$$\left(-\left(\frac{\left(\sqrt{\Psi}+a_1\right)^4}{\Psi^2}-1\right)\lambda^2\left(\sqrt{\Psi}+a_1\right)^2+1\right)=0.$$

This equation has six roots out of which four are complex valued, one is negative and one is positive. We know from Eq. (14) that for $\mathcal{O}(\varepsilon)<\Omega<1$, $\xi_s(\varepsilon)>\xi_s(0)$. Thus, to get the transition correctly from $\Omega = \mathcal{O}(\varepsilon)$ to $\Omega > \mathcal{O}(\varepsilon)$, the positive root is to be chosen. This gives the following solution for

$$\xi_s(\varepsilon) = \sqrt{\varepsilon\Psi} + \sqrt{\varepsilon}\left(-\sqrt{\Psi} + \frac{1}{\sqrt{6}}\sqrt{\frac{\sqrt[3]{12}\left(\left(\Psi^2\left(9+\sqrt{-12\Psi^2\lambda^4+81}\right)\lambda\right)^{2/3}+\Psi^2\lambda^2\sqrt[3]{12}\right)}{\lambda\sqrt[3]{\Psi^2\left(9+\sqrt{-12\Psi^2\lambda^4+81}\right)\lambda}}}\right). \tag{20}$$

4.5. $\xi_a^1(\varepsilon)$

In this subsection, we solve for the coupled wavenumber near the first cut-on of the rigid acoustic duct. Solutions for other $\xi_a^n(\varepsilon)$ may be obtained on similar lines. With $\varepsilon = 0$, this mode cuts-on at $\Omega = \pi/\lambda$. For $0<\varepsilon\ll 1$, we shall look to find a solution close to $\sqrt{\Omega^2-\left(\pi^2/\lambda^2\right)}$ for $\Omega>\frac{\pi}{\lambda}$. The detailed derivation is presented in Table 5.

From Table 5, it is seen that a_1 becomes large at the first cut-on frequency ($\Omega = \pi/\lambda$) and at Ω_c^1, making the asymptotic solution for ξ invalid near these frequencies.

In order to get the solution near $\Omega = \Omega_c^1$ and correctly capture the transition between $\Omega<\Omega_c^1$ and $\Omega>\Omega_c^1$, we assume $\Omega = \Omega_c^1 + \varepsilon\Psi$, where Ψ is an $\mathcal{O}(1)$ quantity, positive for $\Omega>\Omega_c^1$ and negative for $\Omega<\Omega_c^1$. The detailed derivation for $\xi_s(\varepsilon)$ and $\xi_a^1(\varepsilon)$ under this condition is presented in Table 6.

Table 5
Derivation of the asymptotic expression for $\xi_a^1(\varepsilon)$

Substituting $\xi = \sqrt{\Omega^2-\left(\pi^2/\lambda^2\right)} + a_1\varepsilon$ in Eq. (11) and performing a series expansion about $\varepsilon = 0$ we get

$$\left[\frac{\left(\Omega^2-\left(\pi^2/\lambda^2\right)\right)^2}{\Omega^2}-1\right]\lambda^2\sqrt{\frac{\Omega^2\lambda^2-\pi^2}{\lambda^2}}a_1 = 1.$$

The solution for a_1 is

$$a_1 = \frac{\Omega^2\lambda^2}{\left(\sqrt{\left(\Omega^2\lambda^2-\pi^2\right)/\lambda^2}\right)\left(\left(\Omega^2\lambda^2-\pi^2\right)^2-\lambda^4\Omega^2\right)}.$$

$$\Rightarrow a_1 = \frac{\Omega^2\lambda^2}{\underbrace{\left(\sqrt{\left(\Omega^2\lambda^2-\pi^2\right)/\lambda^2}\right)}_{=0 \text{ at cut-on}}\underbrace{\left(\Omega^2\lambda^2-\pi^2-\lambda^2\Omega\right)}_{=0 \text{ at } \Omega_c^1}\left(\Omega^2\lambda^2-\pi^2+\lambda^2\Omega\right)}. \tag{21}$$

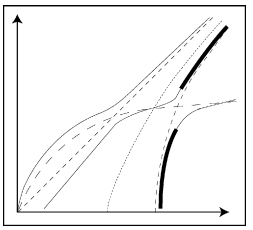

Therefore, $\xi_a^1(\varepsilon) = \sqrt{\Omega^2-\frac{\pi^2}{\lambda^2}} + a_1\varepsilon$ where a_1 is as given above

Table 6
Derivation for $\xi_s(\varepsilon)$ and $\xi_a^1(\varepsilon)$ near Ω_c^1

To find the near-structure solution substitute $\xi = \sqrt{\Omega} + a_1\sqrt{\varepsilon}$ where $\Omega = \Omega_c^1 + \varepsilon\Psi$ in Eq. (11). A series expansion about $\varepsilon = 0$ leads to the following relation for a_1

$$-4\pi^2 a_1^2\lambda^2 - 4\pi^2 a_1^2\lambda^2\sqrt{\frac{\lambda^2+4\pi^2}{\lambda^2}} + \pi^2 + \pi^2\sqrt{\frac{\lambda^2+4\pi^2}{\lambda^2}} = 0 \Rightarrow a_1 = \pm\frac{1}{2\lambda}.$$

Thus, around Ω_c^1 we obtain the following solution for $\xi_s(\varepsilon)$

$$\xi_s(\varepsilon) = \sqrt{\frac{1}{2} + \frac{1}{2}\sqrt{1+4\frac{\pi^2}{\lambda^2}} + \varepsilon\Psi} \pm \frac{1}{2}\frac{\sqrt{\varepsilon}}{\lambda}. \tag{22}$$

For the acoustic cut-on branch around Ω_c^1 we substitute $\xi = \sqrt{\Omega^2 - \frac{\pi^2}{\lambda^2}} + a_1\sqrt{\varepsilon}$ where $\Omega = \Omega_c^1 + \varepsilon\Psi$ in Eq. (11). A series expansion about $\varepsilon = 0$ leads to the following relation for a_1

$$-4\pi^2 a_1^2\lambda^2 - 4\pi^2 a_1^2\lambda^2\sqrt{\frac{\lambda^2+4\pi^2}{\lambda^2}} + \pi^2 + \pi^2\sqrt{\frac{\lambda^2+4\pi^2}{\lambda^2}} = 0 \Rightarrow a_1 = \pm\frac{1}{2\lambda}.$$

Thus, around Ω_c^1 we obtain the solution for $\xi_a^1(\varepsilon)$ as

$$\xi_a^1(\varepsilon) = \sqrt{\left(\frac{1}{2} + \frac{1}{2}\sqrt{1+4\frac{\pi^2}{\lambda^2}} + \varepsilon\Psi\right)^2 - \frac{\pi^2}{\lambda^2}} \pm \frac{1}{2}\frac{\sqrt{\varepsilon}}{\lambda}. \tag{23}$$

We will now fix the proper sign of the second term in Eqs. (22) and (23). From Eqs. (15) and (21) for frequencies below (but not far below) Ω_c^1, $\xi_s(\varepsilon) > \xi_s(0)$ and $\xi_a^1(\varepsilon) < \xi_a^1(0)$ while for frequencies beyond (but not far beyond) Ω_c^1 $\xi_s(\varepsilon) < \xi_s(0)$ and $\xi_a^1(\varepsilon) > \xi_a^1(0)$. Thus to preserve this transition we need to make the following sign choice for asymptotic solutions about Ω_c^1:

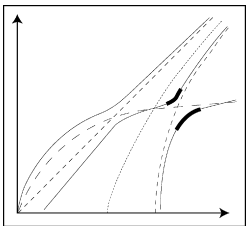

$$\xi_s(\varepsilon) = \sqrt{\frac{1}{2} + \frac{1}{2}\sqrt{1+4\frac{\pi^2}{\lambda^2}} + 4\varepsilon\Psi} + \frac{1}{2}\frac{\sqrt{\varepsilon}}{\lambda} \quad \text{for } \Omega \approx < \Omega_c^1, \tag{24a}$$

$$\xi_s(\varepsilon) = \sqrt{\frac{1}{2} + \frac{1}{2}\sqrt{1+4\frac{\pi^2}{\lambda^2}} + 4\varepsilon\Psi} - \frac{1}{2}\frac{\sqrt{\varepsilon}}{\lambda} \quad \text{for } \Omega \approx > \Omega_c^1, \tag{24b}$$

$$\xi_a^1(\varepsilon) = \sqrt{\left(\frac{1}{2} + \frac{1}{2}\sqrt{1+4\frac{\pi^2}{\lambda^2}} + \varepsilon\Psi\right)^2 - \frac{\pi^2}{\lambda^2}} - \frac{1}{2}\frac{\sqrt{\varepsilon}}{\lambda} \quad \text{for } \Omega \approx < \Omega_c^1, \tag{24c}$$

$$\xi_a^1(\varepsilon) = \sqrt{\left(\frac{1}{2} + \frac{1}{2}\sqrt{1+4\frac{\pi^2}{\lambda^2}} + \varepsilon\Psi\right)^2 - \frac{\pi^2}{\lambda^2}} + \frac{1}{2}\frac{\sqrt{\varepsilon}}{\lambda} \quad \text{for } \Omega \approx > \Omega_c^1. \tag{24d}$$

As $\Psi \to 0^+$, i.e., as we approach Ω_c^1 from the higher frequencies,

$$\xi_s(\varepsilon) \to \sqrt{\frac{1}{2} + \frac{1}{2}\sqrt{1+\frac{4\pi^2}{\lambda^2}}} + \frac{1}{2}\frac{\sqrt{\varepsilon}}{\lambda} \text{ and } \xi_a^1(\varepsilon) \to \sqrt{\left(\frac{1}{2} + \frac{1}{2}\sqrt{1+4\frac{\pi^2}{\lambda^2}}\right)^2 - \frac{\pi^2}{\lambda^2}} - \frac{1}{2}\frac{\sqrt{\varepsilon}}{\lambda}$$

$$= \sqrt{\frac{1}{4} + \frac{1}{2}\sqrt{1+\frac{4\pi^2}{\lambda^2}} + \frac{1}{4}\left(1+\frac{4\pi^2}{\lambda^2}\right) - \frac{\pi^2}{\lambda^2}} - \frac{1}{2}\frac{\sqrt{\varepsilon}}{\lambda} = \sqrt{\frac{1}{2} + \frac{1}{2}\sqrt{1+\frac{4\pi^2}{\lambda^2}}} - \frac{1}{2}\frac{\sqrt{\varepsilon}}{\lambda}. \tag{25}$$

Also, as $\Psi \to 0^-$, i.e., as we approach Ω_c^1 from the lower frequencies,

$$\xi_s(\varepsilon) \to \sqrt{\frac{1}{2}+\frac{1}{2}\sqrt{1+\frac{4\pi^2}{\lambda^2}}-\frac{1}{2}\frac{\sqrt{\varepsilon}}{\lambda}} \quad \text{and} \quad \xi_a^1(\varepsilon) \to \sqrt{\left(\frac{1}{2}+\frac{1}{2}\sqrt{1+4\frac{\pi^2}{\lambda^2}}\right)^2-\frac{\pi^2}{\lambda^2}+\frac{1}{2}\frac{\sqrt{\varepsilon}}{\lambda}}$$

$$= \sqrt{\frac{1}{4}+\frac{1}{2}\sqrt{1+\frac{4\pi^2}{\lambda^2}}+\frac{1}{4}\left(1+\frac{4\pi^2}{\lambda^2}\right)-\frac{\pi^2}{\lambda^2}+\frac{1}{2}\frac{\sqrt{\varepsilon}}{\lambda}} = \sqrt{\frac{1}{2}+\frac{1}{2}\sqrt{1+\frac{4\pi^2}{\lambda^2}}+\frac{1}{2}\frac{\sqrt{\varepsilon}}{\lambda}}. \tag{26}$$

From Eqs. (25) and (26), it is clear that the $\xi_s(\varepsilon)$ branch below Ω_c^1 continues as $\xi_a^1(\varepsilon)$ branch beyond Ω_c^1, while $\xi_a^1(\varepsilon)$ branch below Ω_c^1 continues as $\xi_s(\varepsilon)$ branch beyond Ω_c^1. Both $\xi_s(\varepsilon)$ and $\xi_a^1(\varepsilon)$ branches encounter a jump of $\sqrt{\varepsilon}/\lambda$ at Ω_c^1.

As seen in an earlier subsection, the $\xi_a(\varepsilon)$ branch continues as the $\xi_s(\varepsilon)$ branch beyond coincidence. From the present discussion it is clear, that this $\xi_s(\varepsilon)$ branch continues as $\xi_a^1(\varepsilon)$ for all frequencies beyond Ω_c^1. These continuity arguments hold true for other cut-on branches also. The $\xi_a^n(\varepsilon)$ branch continues as the $\xi_s(\varepsilon)$ branch between Ω_c^n and Ω_c^{n+1} while beyond Ω_c^{n+1} it continues as the $\xi_a^{n+1}(\varepsilon)$ branch.

With $\lambda = 3$ and $\varepsilon = 0.25$, solutions for all branches (i.e., $\xi_s(\varepsilon)$, $\xi_a(\varepsilon)$ and $\xi_a^1(\varepsilon)$) valid for different frequency ranges are plotted in Fig. 5. A schematic of these results was already presented at the beginning of the section in Fig. 3. The legends in Fig. 5 are explained in Table 7. The asymptotic equations used for each non-dimensional frequency range is also shown in Table 7. The valid numerical range for the non-dimensional frequency in any of the asymptotic expressions in Table 7 has to be determined heuristically. This is in the spirit of the asymptotic analysis methodology. For example, the asymptotic solution in Eq. (14) requires Ω to be lesser than unity (by $\mathcal{O}(\varepsilon)$) but does not specify the exact numerical value of Ω upto which the equation can be used. This value is fixed heuristically in trying to obtain smooth continuous solution across the entire range.

In Fig. 5, the coupled dispersion curves are indicated by the following composite curves (1) S0–S1–S2–AP3–AP4, (2) AP1–AP2–S3–S4–S5–AC3–AC4, (3) AC1–AC2-S6–S7. We observe that a single

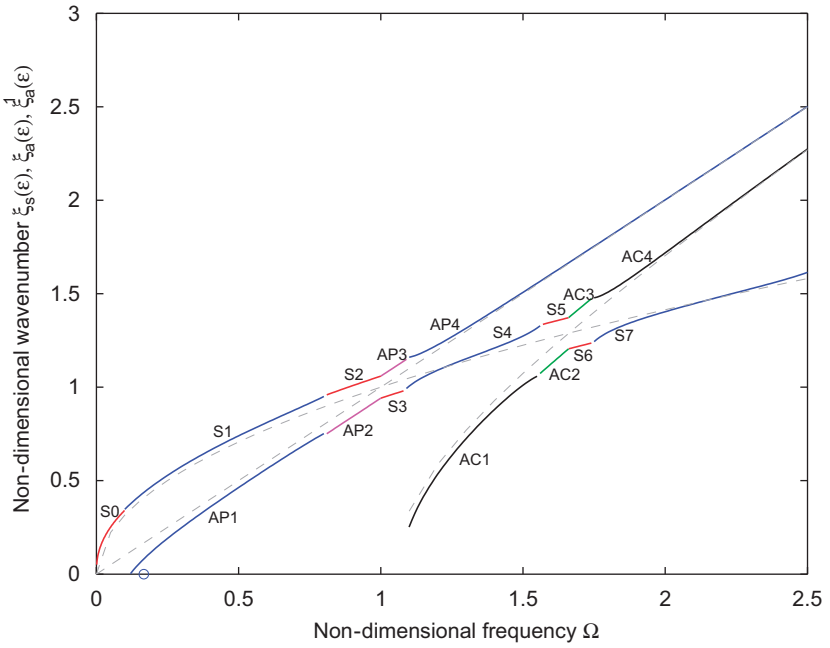

Fig. 5. $\xi_s(\varepsilon)$, $\xi_a(\varepsilon)$ and $\xi_a^1(\varepsilon)$ solutions of Eq. (11) with $\varepsilon = 0.25$ and $\lambda = 3$. Dashed lines represent solutions with $\varepsilon = 0$. Other legends are explained in Table 7.

Table 7
Legends in Fig. 5

Legend	Solution description	Non dimensional frequency range	Equation
○	Acoustic plane-wave cut-on	$\Omega = \mathcal{O}(\varepsilon^{1/2})$	See [1]
S0	Coupled structure	$\Omega = \mathcal{O}(\varepsilon)$	(20)
S1	Coupled structure	$\mathcal{O}(\varepsilon) < \Omega < 1$ (away from 1)	(14)
S2	Coupled structure	$\Omega \approx < 1$	(19a)
S3	Coupled structure	$\Omega \approx > 1$	(19b)
S4	Coupled structure	$1 < \Omega < \Omega_c^1$ (away from both limits)	(15)
S5	Coupled structure	$\Omega \approx < \Omega_c^1$	(24a)
S6	Coupled structure	$\Omega \approx > \Omega_c^1$	(24b)
S7	Coupled structure	$\Omega_c^1 < \Omega < \Omega_c^2$ (away from both limits)	(15)
AP1	Coupled acoustic plane-wave	$0 < \Omega < 1$ (away from both limits)	(16)
AP2	Coupled acoustic plane-wave	$\Omega \approx < 1$	(19c)
AP3	Coupled acoustic plane-wave	$\Omega \approx > 1$	(19d)
AP4	Coupled acoustic plane-wave	$1 < \Omega$ (away from the limits)	(16)
AC1	Coupled acoustic cut-on	$\frac{\pi}{\lambda} < \Omega < \Omega_c^1$ (away from both limits)	(21)
AC2	Coupled acoustic cut-on	$\Omega \approx < \Omega_c^1$	(24c)
AC3	Coupled acoustic cut-on	$\Omega \approx > \Omega_c^1$	(24d)
AC4	Coupled acoustic cut-on	$\Omega_c^1 < \Omega$ (away from the limit)	(21)

composite dispersion curve is made of structural and acoustic segments. For example, (AP1–AP2–S3–S4–S5–AC3–AC4) is made of the planewave segment (AP1–AP2), the structural segment (S3–S4–S5) and the acoustic cut-on segment (AC3–AC4).

It may be noted that the solution tracked in Fig. 5 though approximately continuous is not smooth (i.e., not differentiable) in the transition region. We attribute this to the approximation involved in employing only the first-order correction factor for the asymptotic solutions. It is expected that higher-order terms in the asymptotic expansion if used will lead to better smoothness of the solution. However, this will lead to lengthy expressions, hence we abstain from the use of it. Also, as the objective is to qualitatively understand the nature of the fluid–structure interaction, we feel the first-order correction is sufficient.

In order to compare our results with Fahy [1], his definition of the non-dimensional wavenumber $\chi = \xi/\Omega$ (defined in Table 1) is used instead of ξ in all the asymptotic expressions. The resulting curves are shown in Fig. 6. Figs. 5 and 6 indicate that the branches S0–S1–AP3–AP4, AP1–AP2–S3–S4–S5–AC3–AC4 are in continuity. Qualitatively their nature is identical to that shown in Fig. (113) and Fig. (110a) in Ref. [1]. However, in Ref. [1], solutions were not tracked using a consistent unified asymptotic framework and for some branches, numerical techniques were employed. For these reasons, it is difficult to comprehend the solutions in relation to the *in vacuo* structure or the acoustic plane wave or cut-on wave solutions. Through asymptotic analysis, we realise that the effect of fluid–structure interaction is to introduce perturbations in these well-known solutions. We also get to see how with $\varepsilon \to 0$ these perturbed curves finally collapse to give the classical solutions.

An interesting conclusion borne out from this analysis is that the dispersion curves get perturbed in such a manner that they do not intersect at any point. It is only with $\varepsilon = 0$, that is the case of no coupling, that the dispersion curves corresponding to the structure and the acoustic plane and cut-on waves intersect. For $\varepsilon \neq 0$, at these points of intersection, a gap is formed as is seen from Fig. 5 around the coincidence region and Ω_c^1. At these frequency regions the perturbations are of $\mathcal{O}(\sqrt{\varepsilon})$, while for all other frequencies the perturbations are of $\mathcal{O}(\varepsilon)$.

Fuller and Fahy [7] in their derivation of the dispersion relation for fluid-filled cylindrical shells accounted for the presence of fluid by an additional fluid-loading term in the *in vacuo* structural dispersion relation. In this sense, our approach of viewing the coupled dispersion relation as in Eq. (11) is in line with theirs. They also reported that the coupled wavenumber curves cannot intersect. They offered an explanation based on group velocity of the individual wave modes as to why the intersection cannot occur. The appearance of a gap

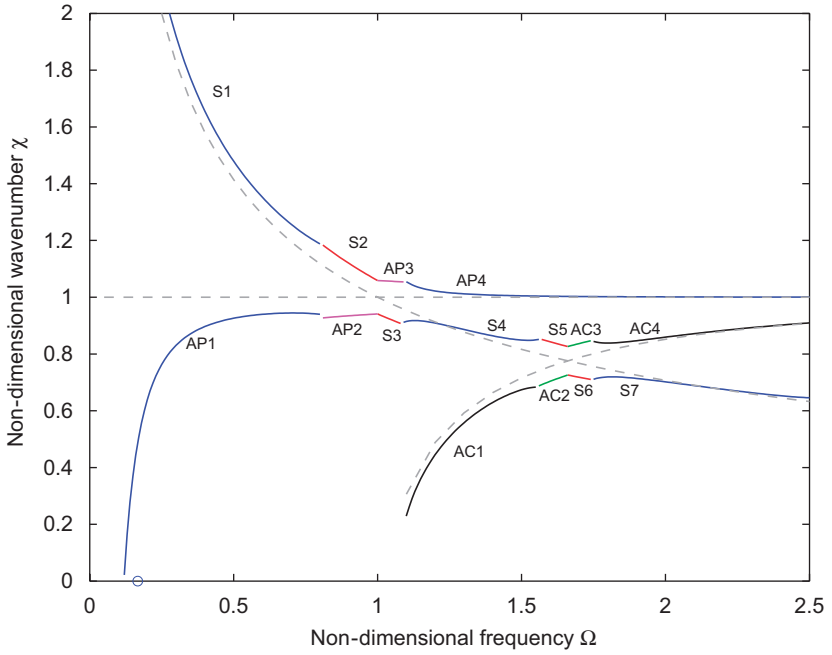

Fig. 6. Asymptotic solutions of Eq. (11) in terms of the non-dimensional wavenumber χ defined in Table 1. Dashed lines represent solutions with $\varepsilon = 0$. Other legends are explained in Table 7.

at the intersection of the dispersion curves was also reported in Cabelli's work [3]. Both the studies [3,7] depict branches of the coupled dispersion curves remaining close to the uncoupled curves and undergoing transitions between the *in vacuo* structural and the uncoupled acoustic solutions.

Similar to Huang et al. [4] and Choi and Kim [6], we have also found that the fluid loading on the structure is given by a coth term for the subsonic case and a cot term for the supersonic case. Huang et al. [4] with their theoretical calculation of fluid wave impedance on the wall in the duct-membrane model showed that if the structural wave is subsonic then the fluid loading is in the form of inertia. Also, if the structural wave is supersonic, then the fluid loading under the long-wavelength assumption is in the form of stiffness.

5. Large fluid-loading parameter

Following the development in the previous sections where the range $0 < \varepsilon \ll 1$ was examined, it is natural to extend the asymptotic analysis to the other extreme range of large ε. Physically, this implies that the mass of the fluid column is much more than the mass of the structure. After the large ε derivations are carried out, we can understand how the solution evolves as ε changes from small to large values.

To model the effect of the large fluid-loading parameter, we substitute $\varepsilon' = 1/\varepsilon$ in Eq. (11) where $0 < \varepsilon' \ll 1$. The non-dimensional equation then becomes

$$\varepsilon'\left(\frac{\xi^4}{\Omega^2} - 1\right)\left(\lambda\sqrt{\Omega^2 - \xi^2}\right) + \cot\left(\lambda\sqrt{\Omega^2 - \xi^2}\right) = 0. \tag{27}$$

With $\varepsilon' = 0$, we have the following solution:

$$\lambda\sqrt{\Omega^2 - \xi^2} = \frac{(2m+1)\pi}{2} \quad \text{where } m = 0, 1, 2, \ldots$$

$$\Rightarrow \Omega^2 - \xi^2 = \left[\frac{(2m+1)\pi}{2\lambda}\right]^2 \Rightarrow \xi = \sqrt{\Omega^2 - \left(\frac{(2m+1)\pi}{2\lambda}\right)^2}. \tag{28}$$

The solution in Eq. (28) corresponds to the cut-on wavenumbers in an acoustic duct with one edge having velocity-zero and the other having a pressure-zero boundary condition. This mode will be referred to as the *pressure-release* mode. Instead of $\varepsilon' = 0$, when $0 < \varepsilon' \ll 1$ the solutions are expected to be perturbations of this pressure-release mode and shall be denoted by $\xi_a'^m$ (called the coupled pressure-release mode). The asymptotic expression for $0 < \varepsilon' \ll 1$ will be derived for the first pressure-release cut-on mode only, i.e., with $m = 0$. Solutions near the other pressure-release cut-ons may similarly be obtained. A detailed derivation of this asymptotic solution is presented in Table 8.

The asymptotic solution in Eq. (29) remains valid for all frequencies other than those near the first pressure-release cut-on (i.e., $\Omega = \frac{\pi}{2\lambda}$), where the correction term of $\mathcal{O}(\varepsilon')$ is seen to grow large. The graph of this solution is presented in Fig. 7 for $\lambda = 3$ and $\varepsilon' = 0.2$ (or $\varepsilon = 5$). The plot indicates that the asymptotic solution turns invalid near $\Omega = \frac{\pi}{2\lambda}$.

Table 8
Asymptotic expansion for large ε around the first pressure-release cut-on mode using Eq. (27)

Substituting, $\xi = \sqrt{\Omega^2 - \left(\frac{\pi}{2\lambda}\right)^2} + a_1\varepsilon' + a_2\varepsilon'^2$ in Eq. (27) and performing a series expansion about $\varepsilon' = 0$ we get

$$\frac{16\pi^2\Omega^4\lambda^4 - 8\pi^4\Omega^2\lambda^2 + \pi^6 - 16\lambda^4\Omega^2\pi^2 + 32\left(\sqrt{(4\Omega^2\lambda^2 - \pi^2)/\lambda^2}\right)a_1\lambda^6\Omega^2}{16\lambda^4\Omega^2\pi^2}\varepsilon' + \mathcal{O}(\varepsilon'^2) = 0.$$

Balancing terms at $\mathcal{O}(\varepsilon')$ we get

$$a_1 = -\pi^2\frac{(16\Omega^4\lambda^4 - 8\Omega^2\lambda^2\pi^2 + \pi^4 - 16\lambda^4\Omega^2)}{32\lambda^6\Omega^2\sqrt{(4\Omega^2\lambda^2 - \pi^2)/\lambda^2}}.$$

$$\text{Thus, } \xi_a'^0(\varepsilon') = \sqrt{\Omega^2 - \frac{\pi^2}{4\lambda^2}} - \pi^2\frac{(16\Omega^4\lambda^4 - 8\Omega^2\lambda^2\pi^2 + \pi^4 - 16\lambda^4\Omega^2)}{32\lambda^6\Omega^2\sqrt{(4\Omega^2\lambda^2 - \pi^2)/\lambda^2}}\varepsilon'. \tag{29}$$

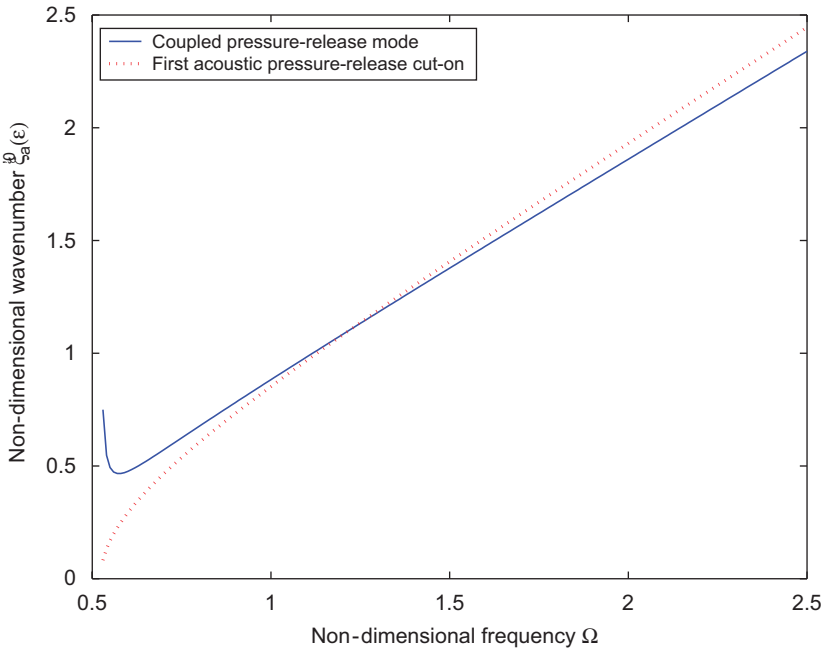

Fig. 7. Solution to the coupled pressure-release mode with $\lambda = 3$ and $\varepsilon' = 0.2$ (or $\varepsilon = 5$).

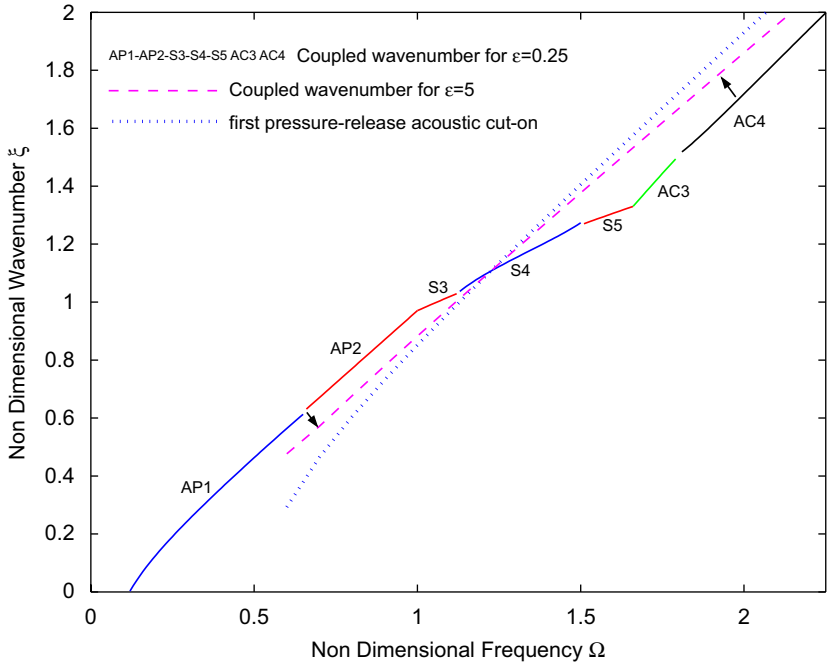

Fig. 8. Transition of the solution of the coupled dispersion Eq. (11) from small ε to large ε for $\lambda = 3$. The solid line is the branch AP1–AP2–S3–S4–S5–AC3–AC4 of Fig. 5 with $\varepsilon = 0.25$ while the dashed line is the solution of Eq. (11) for $\varepsilon = 5$. The arrows indicate the direction of transition of the solution with increasing ε.

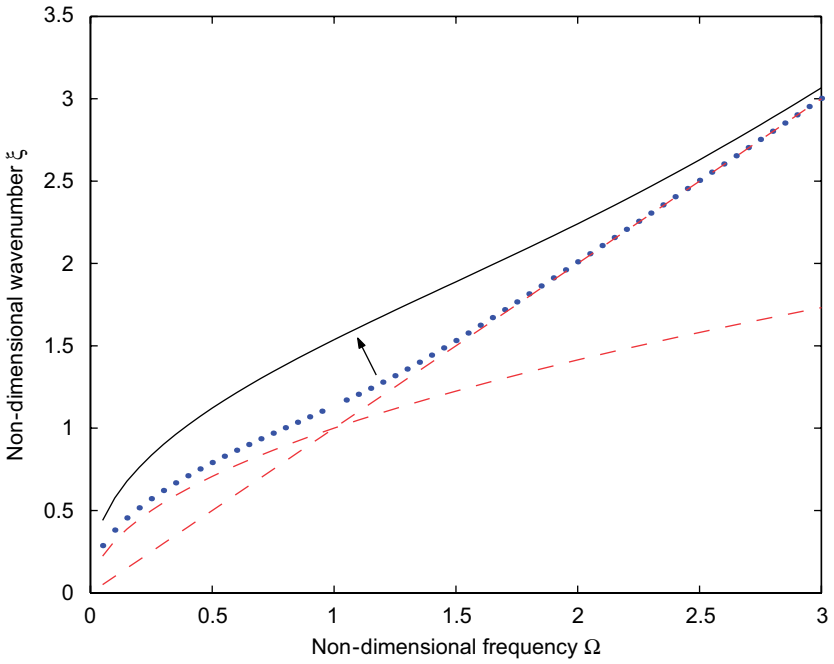

Fig. 9. Numerical solution of Eq. (11) with $\lambda = 3$. Dashed lines represent the *in vacuo* flexural solution and the acoustic plane wave solution. Dotted line represents the solution with $\varepsilon = 1$ and the solid line represents the solution with $\varepsilon = 16$. Arrows indicate the manner in which the solution continuously changes as ε increases.

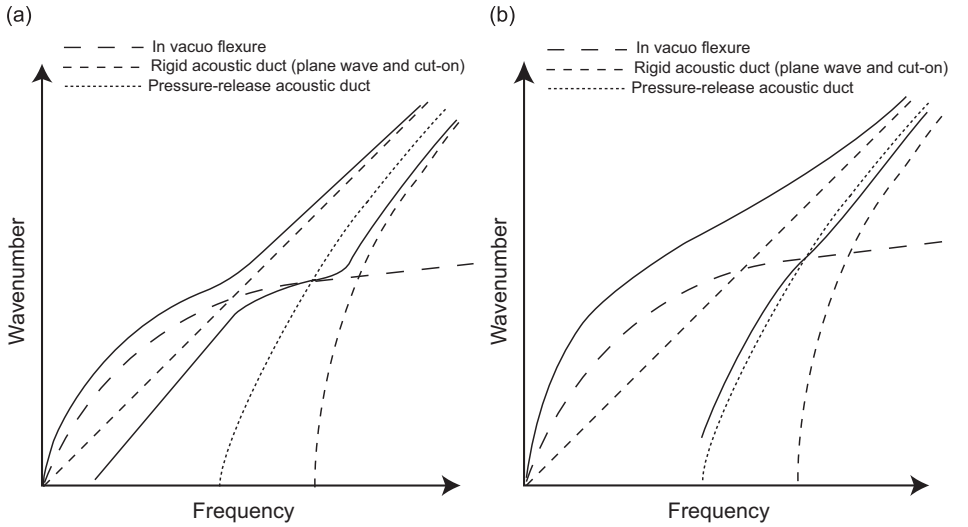

Fig. 10. Schematic of the coupled wavenumber solution (a) small fluid-loading parameter and (b) large fluid-loading parameter.

We are now in a position to understand the behaviour of the coupled free wavenumber as the fluid-loading parameter ε changes continuously from small to large values. In Fig. 8 we replot the solution branch AP1–AP2–S3–S4–S5–AC3–AC4 of Fig. 5 which was valid for small ε, along with the asymptotic solution for large ε obtained through Eq. (29). Two distinct observations can be made based on Figs. 5 and 8. The first is that for small ε, a segment like AP1–AP2 close to the plane wave (or a rigid-walled cut-on mode) makes a transition to a segment like AC3–AC4 near the next rigid-walled cut-on mode through an intermediate zone like S3–S4 which is close to the *in vacuo* structural wavenumber. The second is that as ε is increased from zero to infinity, the entire branch AP1–AP2–S3–S4–S5–AC3–AC4 shifts to $\xi'^0_a(\varepsilon')$ (expression of $\xi'^0_a(\varepsilon')$ is given in Eq. (29)). In Fig. 8 this transition of dispersion curves with increasing ε is indicated by arrows. Physically, this implies a change of the boundary condition from a rigid-wall to a pressure-release as the fluid-loading parameter increases. It may be verified that all the curves $\xi_s(0)$, $\xi'^0_a(0)$, $\xi'^0_a(\varepsilon)$ and AP1–AP2–S3–S4–S5–AC3–AC4 intersect at the same point.

Fahy [1] has presented solutions for large fluid-loading parameter values. The occurrence of solutions near the pressure-release mode for large values of the fluid-loading parameter was shown. In the context of fluid-filled cylindrical shells, numerical studies for large fluid density were presented by Fuller and Fahy [7]. They also demonstrated the transition of the wavenumber branches from a rigid-wall to a pressure-release solution by varying suitable parameters.

As ε increases, the branch S1–S2–AP3–AP4 in Fig. 5 shifts continuously from the uncoupled structural and acoustic curves. We have not been able to find an asymptotic expansion for this branch. We can analytically justify the existence of a branch ξ for Eq. (11) such that $\xi > \Omega$ and $\xi > \sqrt{\Omega}$ for all choices of ε and λ. This has been argued by Fahy. Fig. 9 presents the numerical solution of Eq. (11) for $\lambda = 3$ with $\varepsilon = 1$ and 16. The continuous transition of the solution as ε increases can be identified from this plot. The solution presented by Fahy [1] is in agreement with the above result.

All the derived expressions above have only a first-order correction term. As can be seen, this results in kinks in the corresponding graphs. Higher-order expansions will improve the smoothness of these curves. Hence, for the sake of clarity and for summarizing our findings we present a schematic plot of all the coupled wavenumber branches for small and large values of the fluid-loading parameter in Fig. 10.

6. Conclusions

In this article, analytical expressions are derived for the coupled wavenumbers in a 1-D structural acoustic waveguide. The numerical solutions to the problem were known [1]. The novelty of this article lies in arriving at the same results through analytical expressions derived using asymptotic methods. All types of wavenumber

branches (structural, acoustic planewave and acoustic cut-on) are dealt with comprehensively. Apart from the analytical expressions, the systematic derivation helps to continuously track the wavenumber solutions as the fluid-loading parameter ε is varied from small to large values. A general trend found is that a given composite branch (made up of structural and acoustic segments) transits from a rigid-walled wavenumber solution to a pressure-release wavenumber solution with increase in ε. It is found that at any frequency where two wavenumbers intersect in the uncoupled analysis, there is no more an intersection in the coupled case, but a gap (as in Cabelli's work [3]) is created at that frequency. Finally, this method is simple to implement using a symbolic package and physically insightful.

Acknowledgements

We wish to thank Prof. Anindya Chatterjee, Department of Mechanical Engineering, IISc Bangalore, for introducing us to the interesting subject of Perturbation Methods. Specifically, in this paper, he helped us on some of the trickier asymptotic expansions. We are grateful for his help.

References

[1] F. Fahy, *Sound and Structural Vibration, Radiation, Transmission and Response*, Academic Press, New York, 1989, pp. 259–268 and 136–140.
[2] E.J. Kerschen, J.P. Johnston, Mode selective transfer of energy from sound propagating inside circular pipes to pipe wall vibration, *Journal of Acoustical Society of America* 67 (6) (1980) 1931–1934.
[3] A. Cabelli, The propagation of sound in a square duct with non-rigid side wall, *Journal of Sound and Vibration* 103 (3) (1985) 379–394.
[4] L. Huang, Y.S. Choy, R.M.C. So, T.L. Chong, Experimental study of sound propagation in flexible duct, *Journal of Acoustical Society of America* 108 (2) (2000) 625–631.
[5] S.H. Ko, Sound wave propagation in a two dimensional flexible duct in the presence of an inviscid flow, *Journal of Sound and Vibration* 175 (1994) 279–287.
[6] S. Choi, Y.H. Kim, Sound wave propagation in a membrane duct, *Journal of Acoustical Society of America* 112 (5) (2002) 1749–1752.
[7] C.R. Fuller, F.J. Fahy, Characteristic of wave propagation energy distributions in cylindrical elastic shells filled with fluid, *Journal of Sound and Vibration* 81 (4) (1982) 501–518.
[8] G. Pavic, Vibrational energy flow in elastic circular cylindrical shell, *Journal of Sound and Vibration* 142 (2) (1990) 293–310.
[9] M.K. Au-Yang, The hydrodynamic mass at frequencies above coincidence, *Journal of Sound and Vibration* 86 (2) (1983) 88–292.
[10] A.H. Nayfeh, *Problems in Perturbation*, Wiley, New York, 1985.
[11] E.J. Hinch, *Perturbation Methods*, Cambridge University Press, Cambridge, 1991.
[12] P.M. Morse, K.U. Ingard, *Theoretical Acoustics*, McGrawHill Book Company, New York, 1968, pp. 624–634.
[13] D.G. Crighton, The 1988 Rayleigh Medal Lecture: fluid loading—the interaction between sound and vibration, *Journal of Sound and Vibration* 133 (1) (1989) 1–27.
[14] D.G. Crighton, Fluid–structure Interaction, in: D.G. Crighton, et al. (Eds.), *Modern Methods in Analytical Acoustics*, Springer, Berlin, 1992, pp. 510–523.
[15] N. Peake, S.V. Sorokin, A nonlinear model of the dynamics of a large plate with heavy fluid loading, *Proceedings of Royal Society of London A* 462 (2006) 2205–2224.
[16] C.J. Chapman, S.V. Sorokin, A forced vibration of an elastic plate under significant fluid loading, *Journal of Sound and Vibration* 281 (2005) 719–741.